A NOVEL APPROACH TO THE DESIGN OF OVERSAMPLING COMPLEX-MODULATED DIGITAL FILTER BANKS

Christian Stöcker, Thomas Kurbiel, Daniel Alfsmann, Heinz G. Göckler

Digital Signal Processing Group, Ruhr-University Bochum
D - 44780, Bochum, Germany
phone: +49 (0)234 32-22106, fax: +49 (0)234 32-02106, email: kurbiel@nt.rub.de
web: www.dsv.rub.de

ABSTRACT

This paper addresses the minimisation of the overall disturbances of the output signal of an oversampling DFT subband-coder filter bank. These disturbances are separated into aliasing and imaging. By means of the definitions of these disturbance components, two quadratic functions are derived that are used as objective functions in the design approach. The algorithm optimises in an iterative manner the coefficients of the prototype filters of the analysis and synthesis filter banks. It is proved that the design problem is convex. An efficient implementation of the algorithm is given. A numerical example shows that the output disturbances are highly reduced compared to standard designs.

1. INTRODUCTION

Complex-modulated (DFT) subband coder filter banks (Filter Bank Pairs: FBP) are widely used in multirate signal processing for uniform spectral decomposition [4, 8], where power consumption and, hence, computation is crucial, whilst a specified (output and/or subband) signal quality must strictly be maintained; e.g. mobile systems, hearing aids, etc. In this contribution, the design of non-recursive DFT FBP with approximately perfect reconstruction is revisited, where the signal degradation caused by aliasing and imaging is exclusively controlled by sufficiently high stopband attenuation of the FBP prototype filters. To avoid excessive FIR filter lengths, suitable oversampling of the subband signals by an integer factor is applied [1].

In [2], based on a two-criteria objective function, subband (denoted by inband) aliasing and the FBP output disturbance (so called residual aliasing) are concurrently minimised in the frame of an iterative design procedure: The coefficients of the prototype filters of the analysis and the synthesis filter bank, AFB and SFB, are alternately optimised.

In a different approach [1], the mechanisms of the aliasing and imaging disturbances of oversampling DFT FBP have thoroughly been investigated. As a result, an overall specification of the AFB and SFB prototype filters with frequency-dependent stopband requirements has been derived to maintain a prescribed FBP output signal quality that is essentially independent of subband signal manipulation (hearing aid application).

Stimulated by [1], the two-criteria objective function used in [2] is modified as follows: i) The first criterion measures aliasing in the FBP output signal, which is mainly controlled by the AFB prototype filter stopband rejection, ii) The second criterion measures the imaging disturbance of the FBP output signal, which is solely minimised by optimising the SFB prototype filter coefficients. Similar to [2], the AFB
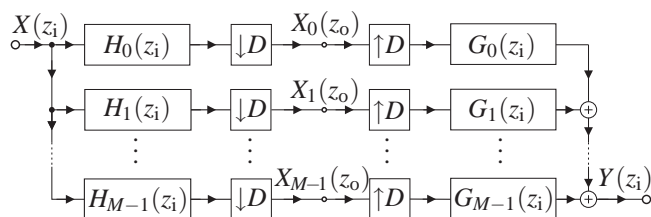
and SFB FIR prototype filters are alternately optimised; thus, the disturbance by aliasing and imaging, respectively, is minimised in an iterative manner.

Subsequently, in sec. 2, the novel two-criteria objective function is derived. The details and an efficient implementation of the optimisation procedure are presented in sec. 3. Illustrative examples in comparison with results obtained according to [2] are shown in sec. 4, followed by concluding remarks.

Figure 1: Oversampling SBC filter bank; $z_\mathrm{o} = z_\mathrm{i}^D$

2. FILTER BANK REPRESENTATION

2.1 Complex-Modulated Filter Banks

In our investigations we assume a uniform, complex-modulated (DFT) M-channel FBP, a subband coder (SBC) filter bank [4, 8], where the prototype filters of the analysis (AFB) and synthesis filter bank (SFB) are real-valued FIR lowpass filters. The vectors of the impulse responses of the AFB and SFB prototype filters are denoted by $\mathbf{h}(n) \leftrightarrow H(e^{\mathrm{j}\Omega})$ and $\mathbf{g}(n) \leftrightarrow G(e^{\mathrm{j}\Omega})$. The respective filter lengths L_h and L_g are generally assumed different. The SBC filter bank applies decimation by the factor $D < M$ such that the oversampling factor $\mathscr{O} = \frac{M}{D} > 1$ is an integer (cf. fig. 1).

The transfer functions of the modulation components of each filter bank are derived from those of the respective AFB and SFB prototype filters [4, 8] by

$$H_m(z_\mathrm{i}) = H(z_\mathrm{i}W_M^m) \text{ and } G_m(z_\mathrm{i}) = G(z_\mathrm{i}W_M^m), \qquad (1)$$

where $W_M = e^{-\mathrm{j}2\pi/M}$, $0 \le m \le M-1$, and z_i is related to the input/output sampling rate f_i of the FBP. The z-transforms of the D-fold downsampled subband signals (AFB output ports) are given by

$$X_m(z_\mathrm{o}) = \frac{1}{D} \sum_{d=0}^{D-1} H\left(z_\mathrm{i}W_M^m W_D^d\right) X\left(z_\mathrm{i}W_D^d\right), \qquad (2)$$

where $z_\mathrm{o} = z_\mathrm{i}^D$. Finally, the transfer properties of the FBP are

completely described by

$$Y(z_i) = \frac{1}{D} \sum_{d=0}^{D-1} X(z_i W_D^d) \sum_{m=0}^{M-1} H(z_i W_M^m W_D^d) G(z_i W_M^m), \quad (3)$$

which represents the z-transform of the overall output signal subject to the input signal.

2.2 Disturbances

In (3), the terms with $d = 0$ represent those desired components that are transferred by the FBP without any non-linear disturbance (aliasing and imaging). Hence, the *distortion function*

$$F_{\text{dist}}(z_i) = \frac{1}{D} \sum_{m=0}^{M-1} H(z_i W_M^m) G(z_i W_M^m) \quad (4)$$

represents the linear distortion of the FBP [4]. In [5] this function is shown to be $\frac{2\pi}{M}$-periodic.

To consider the non-linear disturbance introduced by the FBP, we assume an input signal with a constant (white) spectrum $|X(e^{j\Omega})| \equiv 1$. This non-linear disturbance is measured by the remaining terms, $1 \le d \le D-1$, of (3):

$$F_{\text{alias}}(z_i) = \frac{1}{D} \sum_{d=1}^{D-1} \left[\sum_{m=0}^{M-1} H(z_i W_M^m W_D^d) G(z_i W_M^m) \right] \quad (5)$$

This function is commonly referred to as *aliasing function*, though it contains both types of disturbances that are introduced by the FBP: aliasing and imaging.

Finite stopband attenuation of the AFB prototype FIR filter leads to aliasing as a result of D-fold downsampling (see fig. 1). The only means to reduce the impact of aliasing, is to increase AFB stopband rejection. Similarly, non-linear disturbance of adjacent subbands by imaging is introduced by the SFB. This disturbance can exclusively be controlled by sufficiently high stopband attenuation of the SFB prototype filter. Both types of non-linear disturbance are usually measured and optimised by concurrently minimising the overall error energy according to [2]:
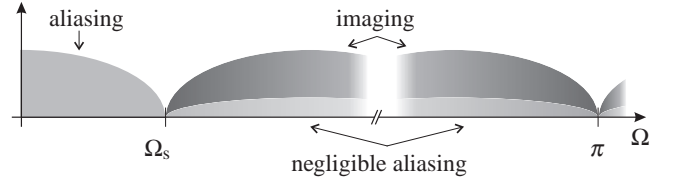
$$\gamma(\mathbf{h}, \mathbf{g}) = \frac{1}{\pi D} \sum_{d=1}^{D-1} \int_0^\pi \left| H(e^{j\Omega} W_D^d) G(e^{j\Omega}) \right|^2 d\Omega \quad (6)$$

Note that, in deriving (6) from (5), it is sufficient to consider only the $m = 0$ term, since (5) is also $\frac{2\pi}{M}$-periodic like (4).

Subsequently, in contrast to (6), we measure and minimise the two types of nonlinear disturbances separately. To develop two separate objective functions, we start with the consideration of the aliasing disturbance with reference to (6) and to fig. 2(a). The dashed line of fig. 2(a) represents the magnitude response of SFB-channel $m = 0$, $|G(e^{j\Omega})|$, collecting all aliasing contributions folded onto the usable spectrum (in $|\Omega| \in [0, \Omega_s]$) of this very subband signal by D-fold downsampling (cf. fig. 1), which pass the stopbands of all frequency-shifted magnitude responses of the AFB prototype filter: $|H(e^{j\Omega} W_D^d)|$, $d = 1, \ldots, D-1$. Hence, the overall aliasing disturbance of the usable spectrum is measured by (6), if the integration interval of (6) is restricted to the passband and transition bands of the SFB prototype filter, $|\Omega| \in [0, \Omega_s]$, as follows:
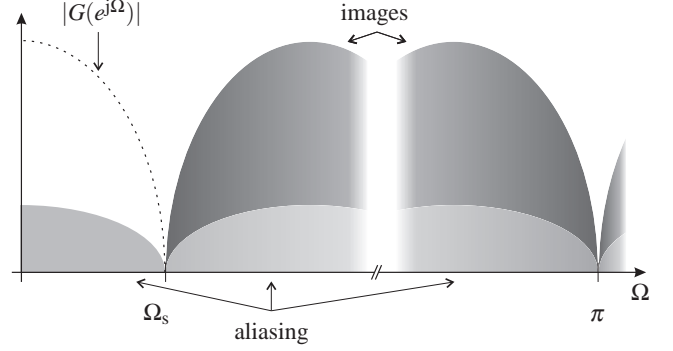
(a) Position of disturbance components behind D-fold upsampling and before SFB filtering

(b) Positions of aliasing and imaging behind SFB filtering

Figure 2: Positions of disturbance components in subband $m = 0$ (M even)

$$\gamma_{\text{A}}(\mathbf{h}, \mathbf{g}) = \frac{1}{\pi D} \sum_{d=1}^{D-1} \int_0^{\Omega_s} \left| H(e^{j\Omega} W_D^d) G(e^{j\Omega}) \right|^2 d\Omega. \quad (7)$$

D-fold upsampling of the subband signals distorted by aliasing (cf. fig. 1) yields the spectral representation depicted in fig. 2(a): Adjacent to the usable spectrum, we observe $D-1$ spectral repetitions of the usable spectrum (images) that disturb all adjacent subband signals after SFB filtering and combination at the FBP output port. Obviously, these images also contain the spectral repetitions of AFB aliasing. Since, however, the energy of these aliasing components is highly reduced by the AFB stopband attenuation, it is neglected in the treatment of imaging subsequently. With this assumption, the overall disturbance due to SFB imaging is again measured by (6), if the integration interval of (6) spans the entire stopband region of the SFB prototype filter, $|\Omega| \in [\Omega_s, \pi]$, as stated by

$$\gamma_{\text{I}}(\mathbf{h}, \mathbf{g}) = \frac{1}{\pi D} \sum_{d=1}^{D-1} \int_{\Omega_s}^\pi \left| H(e^{j\Omega} W_D^d) G(e^{j\Omega}) \right|^2 d\Omega. \quad (8)$$

The aliasing and imaging spectra resulting at the FBP output port are shown in fig. 2(b), confirming the above neglecting of the spectral repetitions of the aliasing contributions.

For input signals with constant (white) spectral density, as assumed here, it is well known that least-squares filter designs yield the optimum output signal-to-noise ratio [4]. Obviously, the optimisation of the AFB and SFB prototype filters subject to the minimisation of the quadratic functions (7) and (8) w.r.t. the respective filter coefficients represents such a least-squares optimisation problem.

Since aliasing is predominantly measured by (7), and imaging is completely comprised by (8), an iterative design procedure that alternately optimises the AFB and SFB prototype filter coefficients, respectively, is most appropriate. Moreover, the frequency domains for both optimisa-

tions, $|\Omega| \in [0, \Omega_s]$ and $|\Omega| \in [\Omega_s, \pi]$, are disjoint. As a consequence, the two sub-optimisations exhibit only small mutual impact on each other. Since, in addition, the optimisation problem is convex (to be shown in sec. 3), fast convergence can be expected.

The two objective functions to be alternately minimised, are given by (7) and (8). Subsequently, these objective functions are analysed and elaborated to a form that, furthermore, considerably reduces the computational load and, thus, the speed of convergence.

3. ITERATIVE FILTER BANK DESIGN

3.1 Minimisation of Aliasing

The squared absolute values of the prototype filters of the AFB and the SFB are given by

$$\left|H(e^{j\Omega})\right|^2 \overset{\text{DTFT}}{\longleftrightarrow} \phi_{\text{hh}}(n) \text{ and } \left|G(e^{j\Omega})\right|^2 \overset{\text{DTFT}}{\longleftrightarrow} \phi_{\text{gg}}(n) \quad (9)$$

where $\phi_{\text{hh}}(n)$ and $\phi_{\text{gg}}(n)$ denote the respective autocorrelation functions [6]. Using (9), we reformulate (7) as a function of the coefficients of the analysis and synthesis prototype filters. Note that

$$\frac{1}{D} \sum_{d=1}^{D-1} \left|H(e^{j\Omega} W_D^d)\right|^2 = \frac{1}{D} \sum_{d=0}^{D-1} \left|H(e^{j\Omega} W_D^d)\right|^2 - \frac{1}{D} \left|H(e^{j\Omega})\right|^2$$

$$\Rightarrow \frac{1}{D} \sum_{d=1}^{D-1} \left|H(e^{j\Omega} W_D^d)\right|^2 \overset{\text{DTFT}}{\longleftrightarrow} w_D(n)\phi_{\text{hh}} - \frac{1}{D}\phi_{\text{hh}}, \quad (10)$$

where

$$w_D(n) = \frac{1}{D} \sum_{d=0}^{D-1} W_D^{-dn} \quad (11)$$

represents the comb sequence [8]. With (10) we get

$$\left|G(e^{j\Omega})\right|^2 \frac{1}{D} \sum_{d=1}^{D-1} \left|H(e^{j\Omega} W_D^d)\right|^2$$

$$= \sum_{n=0}^{L_{\text{conv}}} \phi_{\text{gg}}(n) * \left[\left(w_D(n) - \frac{1}{D}\right)\phi_{\text{hh}}(n)\right] e^{-j\Omega n} \quad (12)$$

where use is made of the DTFT [6], and $L_{\text{conv}} = 2(L_h + L_g) - 3$ is the length of the convolution of $\phi_{\text{hh}}(n)$ with $\phi_{\text{gg}}(n)$. Using the stopband cut-off frequency $\Omega_s = \frac{\pi}{D}$, we reformulate (7):

$$\gamma_A(\mathbf{h}, \mathbf{g}) = \frac{1}{2\pi D} \sum_{d=1}^{D-1} \int_{-\Omega_s}^{\Omega_s} \left|H(e^{j\Omega} W_D^d)G(e^{j\Omega})\right|^2 d\Omega$$

$$= \sum_{n=0}^{L_{\text{conv}}} \phi_{\text{gg}}(n) * \left[\left(w_D(n) - \frac{1}{D}\right)\phi_{\text{hh}}(n)\right] \int_{-\frac{\pi}{D}}^{\frac{\pi}{D}} e^{-j\Omega n} d\Omega$$

$$= \sum_{n=0}^{L_{\text{conv}}} \phi_{\text{gg}}(n) * \left[\left(w_D(n) - \frac{1}{D}\right)\phi_{\text{hh}}(n)\right] \frac{2\pi}{D} \text{si}\left(n\frac{\pi}{D}\right), \quad (13)$$

where $\text{si}(x) = \frac{\sin(x)}{x}$. To set up the minimisation problem subject to the optimisation of coefficients of the AFB prototype filter, we exploit the fact that the Hessian matrix of (13), $\mathbf{H}_A = \frac{\partial \gamma_A(\mathbf{h}, \mathbf{g})}{\partial h_i \partial h_j}$, leads to the objective function

$$\gamma_A(\mathbf{h}, \mathbf{g}) = \mathbf{h}^T \mathbf{H}_A(\mathbf{g})\mathbf{h}. \quad (14)$$

Particularly for practical implementation it is valuable to know the structure of the second derivative of ϕ_{hh} with respect to $\mathbf{h}$. The gradient of ϕ_{hh} is given by

$$\frac{\partial \phi_{\text{hh}}(n)}{\partial h_\nu} = h(\nu - n) + h(\nu + n) = \frac{\partial \phi_{\text{hh}}(-n)}{\partial h_\nu}, \quad (15)$$

where $h_\nu = h(\nu)$. Note the structure of the gradient:

$$\frac{\partial \phi_{\text{hh}}(n)}{\partial h_0} = [h_{L_h-1} \cdots h_1 \ 2h_0 \ h_1 \cdots h_{L_h-1}]$$

$$\frac{\partial \phi_{\text{hh}}(n)}{\partial h_1} = [\ 0 \ \cdots h_0 + h_2 \ 2h_1 \ h_0 + h_2 \cdots \ 0 \ ]$$

$$\vdots \qquad\qquad\qquad \vdots$$

As a result, the terms of $\frac{\partial \phi_{\text{hh}}}{\partial h_i \partial h_j}$ can be written as follows:

$$\frac{\partial \phi_{\text{hh}}(n)}{\partial h_0 \partial h_0} = [0 \ \cdots \ 0 \ 0 \ 2 \ 0 \ 0 \ \cdots \ 0]$$

$$\frac{\partial \phi_{\text{hh}}(n)}{\partial h_0 \partial h_1} = [0 \ \cdots \ 0 \ 1 \ 0 \ 1 \ 0 \ \cdots \ 0]$$

$$\vdots \qquad\qquad\qquad \vdots$$

$$\frac{\partial \phi_{\text{hh}}(n)}{\partial h_1 \partial h_0} = [0 \ \cdots \ 0 \ 1 \ 0 \ 1 \ 0 \ \cdots \ 0]$$

$$\frac{\partial \phi_{\text{hh}}(n)}{\partial h_1 \partial h_1} = [0 \ \cdots \ 0 \ 0 \ 2 \ 0 \ 0 \ \cdots \ 0]$$

$$\vdots \qquad\qquad\qquad \vdots$$

$$(16)$$

Note that the second derivative of ϕ_{hh} with respect to $\mathbf{h}$ is independent of the coefficients of the AFB prototype filter. This additionally shows that (14) represents a quadratic optimisation problem. Considering (7), negative values are excluded by definition which consequently makes this objective function strictly convex. Hence, a unique solution always exists.

3.2 Minimisation of Imaging

To reformulate (8) to a quadratic minimisation problem subject to the optimisation of the coefficients of the SFB prototype filter, we can similarly proceed as in sec. 3.1. The objective function is then given by

$$\gamma_I(\mathbf{h}, \mathbf{g}) = \sum_{n=0}^{L_{\text{conv}}} \phi_{\text{gg}}(n) * \left[\left(w_D(n) - \frac{1}{D}\right)\phi_{\text{hh}}(n)\right] \cdot$$

$$\left(2\pi \text{si}(n\pi) - \frac{2\pi}{D}\text{si}\left(n\frac{\pi}{D}\right)\right) \quad (17)$$

With the Hessian matrix of (17), $\mathbf{H}_I = \frac{\partial \gamma_I(\mathbf{h}, \mathbf{g})}{\partial g_i \partial g_j}$, we finally define the respective optimisation problem

$$\gamma_I(\mathbf{h}, \mathbf{g}) = \mathbf{g}^T \mathbf{H}_I(\mathbf{h})\mathbf{g}. \quad (18)$$

The second derivative of ϕ_{gg} with respect to $\mathbf{g}$ has a similar structure compared to the one in (16) and is also independent of $\mathbf{g}$; (8) takes on only positive values by definition, thus (18) again represents a strictly convex optimisation problem.

3.3 Constraints to the Optimisation

The prototypes of the FBP are to be designed under the condition that the resulting distortion function (4) is approximatly a linear-phase allpass function. The desired distortion function can thus be stated as

$$F_d(e^{j\Omega}) = e^{-j\Omega\tau_d}, \quad (19)$$

where $\tau_{\mathrm{d}} = lM$ with $l \in \mathbb{N}$ is the desired delay [5]. Hence for every step of optimisation the constraints are defined by

$$\left| F_{\mathrm{dist}}(e^{\mathrm{j}\Omega}) - F_{\mathrm{d}}(e^{\mathrm{j}\Omega}) \right| \leq \varepsilon(\Omega) \qquad \forall \Omega \in \left[0, \frac{\pi}{M}\right], \quad (20)$$

where the restricted frequency range exploits the $\frac{2\pi}{M}$-periodicity of the distortion function. With the real rotation theorem [3] it is possible to estimate the upper bound of a complex value by its real part. Employing this theorem to (20) we get

$$\mathscr{R}\left\{ F_{\mathrm{dist}}(e^{\mathrm{j}\Omega}) e^{\mathrm{j}\alpha} \right\} \leq \cos(\alpha - \Omega\tau_{\mathrm{d}}) + \varepsilon(\Omega)$$
$$\forall \Omega \in \left[0, \frac{\pi}{M}\right] \text{ and } \forall \alpha \in [0, 2\pi] \quad (21)$$

To write (21) as a system of linear inequalities, the left hand side has to be reformulated as a function of the respective prototype filter coefficients, to be optimised. In [5] it is shown that $F_{\mathrm{dist}}(e^{\mathrm{j}\Omega})$ can be written as

$$F_{\mathrm{dist}}(e^{\mathrm{j}\Omega}) = \mathscr{O} \sum_{n=0}^{L_{\mathrm{h}}+L_{\mathrm{g}}-2} s(n) w_M(n) e^{-\mathrm{j}\Omega n}$$
$$= \mathscr{O} \sum_{n=0}^{\lfloor \frac{L_{\mathrm{h}}+L_{\mathrm{g}}-2}{M} \rfloor} e^{-\mathrm{j}\Omega nM} s(nM) \quad (22)$$

where $\mathbf{s} = \mathbf{h} * \mathbf{g}$ and $w_M(n)$ is defined by (11) with $D = M$.

The number of constraints N_{constr} depends on the number of discrete frequency points N_{D} over $\left[0, \frac{\pi}{M}\right]$, and on the chosen grid N_α over the 2π-period realising the real-rotation theorem:

$$N_{\mathrm{constr}} = N_{\mathrm{D}} \cdot N_\alpha. \quad (23)$$

3.4 Algorithm

Finally, the complete algorithm for FBP prototype filters design consists of three steps:

1 Initialisation Define initial filters $\mathbf{h}$ and $\mathbf{g}$ with the respective lengths L_{h} and L_{g}. Set the costs $c_{\mathrm{h}}(0)$ and $c_{\mathrm{g}}(0)$ that represent the value of the objective functions to an arbitrarily high value and the counter variable to $k = 1$.

2 Optimise analysis filter Start optimisation of (14) under the constraints (21). Set $c_{\mathrm{h}}(k) = \gamma_{\mathrm{A}}(\mathbf{h}, \mathbf{g})_{|\mathbf{h}=\mathbf{h}_{\mathrm{opt}}}$ and check if $c_{\mathrm{h}}(k-1) - c_{\mathrm{h}}(k) \geq \kappa c_{\mathrm{h}}(k-1)$ is true, where κ is a small number (e.g. $\kappa = 10^{-4}$). Then set $\mathbf{h} = \mathbf{h}_{\mathrm{opt}}$ and continue with step 3, otherwise stop the algorithm.

3 Optimise synthesis filter Start optimisation of (18) under the constraints (21). Set $c_{\mathrm{g}}(k) = \gamma_{\mathrm{I}}(\mathbf{h}, \mathbf{g})_{|\mathbf{g}=\mathbf{g}_{\mathrm{opt}}}$ and check if $c_{\mathrm{g}}(k-1) - c_{\mathrm{g}}(k) \geq \kappa c_{\mathrm{g}}(k-1)$ is true. Then set $\mathbf{g} = \mathbf{g}_{\mathrm{opt}}$, $k = k+1$ and continue with step 2, otherwise stop the algorithm.

Consider that the initial filters can be chosen randomly because of the convexity of the respective optimisation problems. Further more the algorithm always converges to the unique solution of the design approach. The algorithm stops if either in step 2 or 3 the relative improvement ranges below the factor κ.
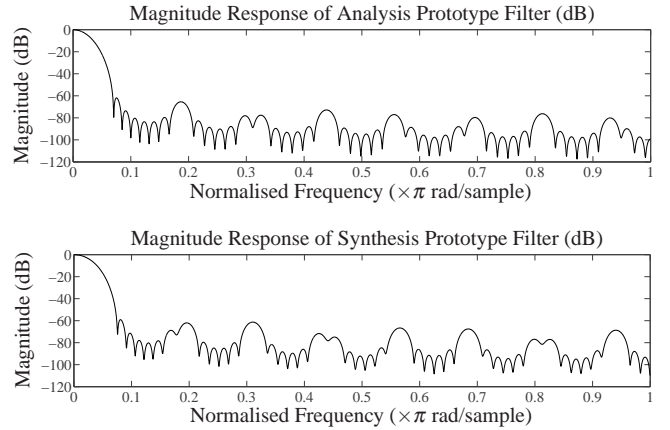

Figure 3: Design result for a SBC filter bank with $M = 64$, $D = 16$ and filter lengths $L_{\mathrm{h}} = L_{\mathrm{g}} = 85$

4. DESIGN EXAMPLE

4.1 Discussion of a Design Result

The following design result is a solution for a FBP with $M = 64$ channels and a downsampling/interpolation factor $D = 16$ so that the oversampling factor $\mathscr{O} = 4$. Initially, the lengths of the filters of the AFB and SFB were set to $L_{\mathrm{h}} = L_{\mathrm{g}} = 85$. The constraint (20) of the distortion function is chosen to $\varepsilon(\Omega) = 0.01$. Furthermore, the desired group delay was set to $\tau_{\mathrm{d}} = M$.

During the design iterations the number of equi-angular points $\alpha \in [0, 2\pi]$ used in (21) to implement the real rotation theorem is initially set to $N_\alpha = 4$ and always doubled from iteration to iteration. Hence, due to (23), the number of constraints was kept low initially. Consequently, this procedure accelerates convergence, considering that the initial filters could be random vectors. In this case the algorithm stopped after four iterations (i.e. two optimisations of each prototype filter).

The obtained prototype filters lead to an aliasing (7) of -183.91 dB and an imaging (8) of -175.65 dB. These results are a significant improvement compared to linear-phase equiripple designs [7] using the same filter lengths, and with approximately the same quality of distortion function and overall group delay. These filters contribute both aliasing and imaging of -108.19 dB.

Note that both responses exhibit a remarkable resemblance with Nyquist(D)filters (D-th band filters [4]) with interlaced stopband domains of higher and lower rejection (i.e. don't care regions), where D represents the decimation/interpolation factor. Considering the AFB response, those aliasing components that are folded onto the passband centres of the respective SFB filters are best captured by the SFB and, hence, must maximally be attenuated by the AFB prototype. These aliasing components are allocated about $\Omega_d = 2\pi\frac{d}{D}$, $d = 1, \ldots, D-1$, where the AFB stopband response exhibits the highest rejection. As to the synthesis filter bank, an SFB can, in principle, be derived from its dual AFB by transposition [4]. In the case of our SFB design, this is reflected by the fact that the SFB prototype filter magnitude response highly resembles that of the corresponding AFB; cf. fig. 3. For a more detailed discussion refer to [1].

The design results have also notable characteristics con-

used parameters: $L_\mathrm{h} = L_\mathrm{g} = 85$ $\tau_\mathrm{d} = 64$, $\varepsilon(\Omega) = 0.086$ dB		measures from [2] in dB		novel measures in dB		number of iterations	ΔF_dist in dB
		inband aliasing	residual aliasing (6)	aliasing (7)	imaging (8)		
novel approach		-158.38	-172.81	-183.91	-175.65	4	0.086
approach according to [2]	$v = M$	-173.29	-171.40	-175.49	-179.89	6	0.086
	$v = 2M$	-174.28	-170.37	-173.79	-180.10	6	0.086
	$v = 3M$	-174.72	-169.72	-172.81	-180.18	6	0.086

Table 1: Summary of the comparison with the design method proposed in [2]

cerning the FBP group delay, which is approximately constant within the passband. This group delay oscillates between 63.38 and 64.61 samples, which shows that the initial specification of $\tau_\mathrm{d} = M = 64$ is well maintained.

4.2 Comparison to an Alternative Design Approach

The design approach proposed in [2] uses a weighting factor v while optimising the inband and residual aliasing. This factor defines the weight of the inband aliasing related to that of the residual aliasing of the objective function. In the following, three design results of this algorithm are compared with our design results. To assure a fair comparison, all above specified parameters are identical for both design approaches.

A summary of the comparison of the design approaches is given in table 1, and discussed below. The obtained results of both methods are evaluated with the measures of [2] as well as with those defined in this paper for aliasing (7) and imaging (8). Furthermore the number of required iteration steps and the maximum deviation of the distortion function ΔF_dist are given.

Considering the proposed separate measurement of the overall aliasing (7) and imaging (8) energy at the FBP output port, our design yields somewhat better results than that of [2], regardless of the weighting factor v. This is further confirmed by the non-coherent combination of both disturbances at the FBP output port, which is best reflected by the "residual aliasing" column of table 1, since it represents the sum of the novel defined measures. On the other hand, the aliasing energy contained in the subbands (inband aliasing) is smaller with the design approach of [2]. This is due to the fact that in our approach aliasing is solely measured at the FBP output port, whereas, in [2], inband aliasing is directly minimised in the FBP subbands.

To perform the comparison of our design results with those obtained according to [2], the latter being likewise constrained by condition (20) has also been implemented by applying the real rotation theorem [3] with doubling of N_α from one iteration step to the next one. As a result, the computational loads of both design approaches grow exponentially with the number of iterations. Hence, a small number of iterations is highly desirable. As to be seen from table 1, this is better achieved by our design procedure as a result of the disjoint frequency domains of the alternating sub-optimisations.

5. CONCLUSION

We have proposed a novel iterative approach to the design of oversampling uniform DFT filter bank pairs (FBP) of the SBC type that approximately achieve perfect reconstruction. In view of extensive subband signal manipulation (e.g. in hearing aid applications), solely the magnitude responses of

the AFB and SFB are matched, whilst aliasing compensation is not exploited.

The AFB FIR prototype filter is optimised by minimising the overall aliasing energy collected in the passband and the transition bands $[-\Omega_\mathrm{s}, \Omega_\mathrm{s}]$ of the prototype. Contrary, the SFB parameters are optimised by minimising the overall energy of images allocated throughout the stopband frequency range $[\Omega_\mathrm{s}, 2\pi - \Omega_\mathrm{s}]$ of the SFB prototype filter. Since the frequency domains of the alternating AFB and SFB optimisations are disjoint, the proposed design approach requires only few iterations. Moreover, some novel ideas are exploited to speed up the kernel of the optimisation procedure. Most importantly, the design approach is convex and, thus, the optimum result is independent of any initial solution.

Our design results compare well with those obtained according to [2], if the overall disturbance caused by aliasing (7) and imaging (8), or the residual aliasing of [2], respectively, is considered. Nevertheless, further research shall clarify, how aliasing (7) and imaging (8) disturbances can better be balanced, for instance, by choosing different lengths of the AFB and SFB prototype filters, and whether or not the overall disturbance can still be reduced by this action.

REFERENCES

[1] D. Alfsmann, H. G. Göckler, T. Kurbiel "Frequency Domain Constraints to Oversampling Filter Bank Systems in Hearing Aids to Ensure a Prescribed Output Signal-to-Distortion Ratio", *J. Advances Sign. Process.*, accepted for public.

[2] H. H. Dam, S. Nordholm, A. Cantoni, and J. M. de Haan, "Iterative Method for the Design of DFT Filter Bank", *IEEE Trans. Circuits Syst. II*, vol. 51, pp. 581–586, Nov. 2004.

[3] K. Glashoff, K. Roleff, "A New Method for Chebyshev Approximation of Complex-Valued Functions", *Mathematics of Computation*, vol. 36, pp. 233–239, Jan. 1981.

[4] H. G. Göckler, A. Groth *Multiratensysteme*, J. Schlembach Fachverlag, Wilburgstetten, 2004.

[5] T. Kurbiel, H.G. Göckler, D. Alfsmann, "Oversampling Complex-Modulated Digital Filter Bank Pairs Suitable for Extensive Subband-Signal Amplification", *J. Advances Sign. Process.*, accepted for public.

[6] A. V. Oppenheim, R. W. Schafer *Discrete-time signal processing*. Address: Prentice Hall, Inc., Englewood Cliffs, 1999.

[7] T. W. Parks, C. S. Burrus *Digital Filter Design*, John Wiley & Sons, Inc., New York, 1987.

[8] P. P. Vaidyanathan *Multirate Systems and Filter Banks*, Prentice Hall, Inc., Englewood Cliffs, 1993.